# A short binding site in the KPC1 ubiquitin ligase mediates processing of NF-κB1 p105 to p50: A potential for a tumor-suppressive PROTAC

Gilad Goldhirsh[a,b], Yelena Kravtsova-Ivantsiv[a,b], Gandhesiri Satish[c], Tamar Ziv[d], Ashraf Brik[c,1], and Aaron Ciechanover[a,b,1]

[a]Rappaport Faculty of Medicine and Research Institute, Technion–Israel Institute of Technology, Haifa 3109601, Israel; [b]Rappaport Technion Integrated Cancer Center, Technion–Israel Institute of Technology, Haifa 3109601, Israel; [c]Schulich Faculty of Chemistry, Technion–Israel Institute of Technology, Haifa 3200008, Israel; and [d]Smoler Proteomics Center, Faculty of Biology, Technion–Israel Institute of Technology, Haifa 3200003, Israel

Contributed by Aaron Ciechanover, October 20, 2021 (sent for review September 19, 2021; reviewed by Ivan Dikic and Moshe Oren)

**Nuclear factor κB (NF-κB) is an important transcriptional regulator that is involved in numerous cellular processes, including cell proliferation, immune response, cell survival, and malignant transformation. It relies on the ubiquitin–proteasome system (UPS) for several of the steps in the concerted cascade of its activation. Previously, we showed that the ubiquitin (Ub) ligase KPC1 is involved in ubiquitination and limited proteasomal processing of the NF-κB1 p105 precursor to generate the p50 active subunit of the "canonical" heterodimeric transcription factor p50–p65. Overexpression of KPC1 with the generation of an excessive amount of p50 was shown to suppress tumors, an effect which is due to multiple mechanisms. Among them are suppression of expression of programmed cell death-ligand 1 (PD-L1), overexpression of a broad array of tumor suppressors, and secretion of cytokines which results in recruitment of suppressive immune cells into the tumor. Here, we show that the site of KPC1 to which p105 binds is exceptionally short and is made up of the seven amino acids WILVRLW. Attachment of this short stretch to a small residual part (∼20%) of the ligase that also contains the essential Really Interesting New Gene (RING)-finger domain was sufficient to bind p105, conjugate to it Ub, and suppress tumor growth in an animal model. Fusion of the seven amino acids to a Von Hippel–Lindau protein (pVHL)-binding ligand (which serves as a "universal" ligase for many proteolysis-targeting chimeras; PROTACs) resulted in a compound that stimulated conjugation of Ub to p105 in a cell-free system and its processing to p50 in cells and restricted cell growth.**

ubiquitin–proteasome | KPC1 | NF-κB | p50 | PROTAC

Nuclear factor κB (NF-κB) is a family of transcription factors which coordinate a broad array of cellular processes such as cell death and survival, differentiation and proliferation, and immune and inflammatory responses (1). Its activation is a multistep process, initiated by a broad array of extracellular cues, and mediated to a large extent by the ubiquitin–proteasome system (UPS) (2, 3). Up-regulation of NF-κB is frequently observed in a variety of tumors, and probably plays a role in malignant transformation. The mechanism(s) that underlies the protumorigenic activity of NF-κB involves up-regulation of expression of proproliferative and antiapoptotic genes, as well as stimulation of the inflammatory process (1, 4, 5).

The NF-κB family consists of five different proteins—three Rel proteins (RelA, RelB, and cRel) and two proteins, p50 and p52, which are derived from limited, UPS-mediated processing of longer precursors, p105 (NF-κB1) and p100 (NF-κB2), respectively. Members of the two groups generate different heterodimers which trigger unique transcriptional programs (2–4). In most cases, the tumorigenicity is related to the p50–p65 dimer (6–8).

Although NF-κB is generally described as oncogenic, a few studies have shed light on its tumor-suppressive activities which are mediated mainly by p50 (9). For example, in pancreatic cancer cells, IκB kinase α (IKKα) down-regulation results in suppression of expression of Skp2, a component of the ubiquitin (Ub) ligase that degrades the cell-cycle suppressor $p27^{Kip}$. This results in up-regulation of $p27^{Kip}$, which is tumor-suppressive. Part of the effect is due to the fact that the down-regulation of IKKα stimulates switching of the NF-κB dimers occupying the promoter of Skp2 from the tumor promoter p52–RelB site to the tumor-suppressive p50–RelB site, which results in inhibition of Skp2 expression (10). Another study shows that NF-κB1 knockout (KO) cells accumulate alkylating agent–induced mutations, and NF-κB1 KO mice are more susceptible to developing lymphomas due to the DNA damage caused by the mutating agents (11). An interesting example is the Ub ligase RNF20 that exerts a tumor-suppressive activity mediated via monoubiquitination of H2B on lysine 120 (H2Bub1). The ligase activity results in a switch between p50–p65– and p50–p50–containing NF-κB dimers that occupy DNA, reducing the ability of tumor necrosis factor (TNF) to up-regulate expression of a subset of inflammation-associating genes (12).

In a different study, our laboratory identified the Ub ligase KPC1 as the enzyme that ubiquitinates p105, resulting in its limited processing to the p50 subunit. Overexpression of p50 resulted in a strong tumor-suppressive effect mediated by two

## Significance

**Accumulation of abnormal proteins underlies the mechanisms of numerous diseases such as malignancies and neurodegeneration. A recent development makes use of the UPS to remove such proteins. Small molecules (PROTACs) that are made of two heads—one that binds to a "universal" Ub ligase and the other that binds to the target substrate—bring the two together, which results in ubiquitination and subsequent proteasomal degradation of the target. We designed a PROTAC made of the pVHL ligase ligand and the short site of the KPC1 ligase that binds the p105 NF-κB precursor. The PROTAC mimics the enzymatic activity of the native KPC1 and can therefore serve as a prototype for the development of a tumor-suppressive drug.**

Author contributions: G.G., Y.K.-I., T.Z., A.B., and A.C. designed research; G.G., Y.K.-I., and T.Z. performed research; G.G., Y.K.-I., G.S., T.Z., and A.B. contributed new reagents/analytic tools; G.G., Y.K.-I., T.Z., A.B., and A.C. analyzed data; and G.G., Y.K.-I., G.S., T.Z., A.B., and A.C. wrote the paper.

Reviewers: I.D., Goethe-Universitat Frankfurt am Main; and M.O., Weizmann Institute of Science.

Competing interest statement: A.C. and M.O. are coauthors on a 2018 multiauthor apoptosis nomenclature-proposing article (https://doi.org/10.1038/s41418-017-0012-4).



[1]To whom correspondence may be addressed. Email: abrik@technion.ac.il or aaroncie@tx.technion.ac.il.

This article contains supporting information online at http://www.pnas.org/lookup/suppl/doi:10.1073/pnas.2117254118/-/DCSupplemental.

Published December 3, 2021.

main mechanisms: 1) up-regulation of various tumor suppressors (13); and 2) modulation of the tumor microenvironment by recruiting and activating the immune system: An excess of KPC1 or p50 up-regulates expression of CCL3, CCL4, and CCL5, which are proinflammatory chemokines, which in turn recruit to the tumor natural killer cells and macrophages. Also, p50 down-regulates the expression of the immune checkpoint programmed cell death-ligand 1 (PD-L1) (14). It should be noted that since p50 does not have a transactivation domain, and since the activity of the putative p50–p50 homodimer stimulates transcription of tumor suppressors (13) and chemokines (14), the homodimer has to be joined by a component that has a transactivation domain.

In the current study, we identified the site on KPC1 that binds p105. The site is exceptionally short and is made up of seven amino acids—WILVRLW. A truncated protein that contains the C-terminal domain of KPC1 (~20% of wild-type [WT] KPC1) to which the seven amino acids are fused preserves the ability to interact with and ubiquitinate NF-κB1 p105. Importantly, this small protein preserves the tumor-suppressive activity of WT KPC1 in a xenograft tumor model. Interestingly, sites of Ub ligases that bind their cognate substrates are rather long. For example, the interaction site of KPC1 which regulates the degradation of p27 at the G1 phase of the cell cycle spans 766 amino acids at the N-terminal part of the molecule (15). Another example is the interaction site of MDM2 with p53. It was shown that deletion of the N-terminal 61 amino acids of the ligase abrogated its interaction with the tumor suppressor (16, 17).

Identification of the short binding site prompted us to generate a proteolysis-targeting chimera (PROTAC) made of these seven amino acids fused to a Von Hippel–Lindau protein (pVHL)-binding ligand. PROTACs are small, cell-penetrable molecules with two heads. One head binds to a "universal" ligase such as Cereblon or pVHL, whereas the other binds to the target substrate. Bringing the substrate into close vicinity with the ligase results in its ubiquitination and subsequent proteasomal degradation, which enables one to design small molecules that potentially can degrade any protein at will (18, 19). The PROTAC we designed was able to mediate p105 ubiquitination in a cell-free system, stimulate p105 processing to p50 in cells, and restrict cell division. Taken together, the PROTAC has the potential to become a tumor-suppressive drug.

## Results

**Amino Acids WILVRLW (residues 968–974) in the KPC1 Sequence Are Necessary for the Interaction of the Ligase with p105.** In a previous study, we identified KPC1 as the E3 Ub ligase that mediates ubiquitination and proteasomal processing of the NF-κB1 p105 to the p50 active subunit of the transcriptional regulator (13). The excess of the p50 generated a strong tumor-suppressive activity which is mediated via several independent mechanisms (13, 14). We further showed that p105 binds to the ligase via its ankyrin repeat domain (13). However, the site in KPC1 that recognizes p105 has remained elusive.

To identify the region in KPC1 that binds NF-κB1 p105, we systematically generated a collection of truncated species of the ligase fused to a FLAG tag (Fig. 1 *A*, *i*, *B*, *i*, and *C*, *i*) and monitored their interaction with p105. HEK293 cells were transfected with a complementary DNA (cDNA) coding for p105-HA (hemagglutinin) and cDNAs coding for the WT and truncated species of KPC1-FLAG.

We examined the interaction of the KPC1-truncated proteins with p105 in coimmunoprecipitation assays (Fig. 1 *A*, *ii–iv*, *B*, *ii* and *iii*, and *C*, *ii–iv*). p105 coprecipitated with the following KPC1 truncated proteins: WT KPC1-FLAG (Fig. 1 *A*, *ii–iv*, lanes 1), KPC1Δ1–967-FLAG (lanes 4), KPC1Δ1041–1061-FLAG (lanes 6), and WILVRLW-KPC1Δ1–1039-FLAG (lanes 7). This experiment strongly suggested that the domain in KPC1 that binds p105 spans residues 968 to 974 (WILVRLW). Importantly, we showed that KPC1 variants that lack the first 1,039 residues (Fig. 1 *A*, *i*, construct 7) or the first 1,254 residues (Fig. 1 *C*, *i*, construct 2), but to which the sequence WILVRLW was fused to their N terminus, bind to p105 (Fig. 1 *A*, *ii–iv*, lanes 7, and *C*, *ii–iv*, lanes 2, respectively). Importantly, the two truncated species still contained their Really Interesting New Gene (RING)-finger domain necessary for recruitment of the E2 (Ub-conjugating enzyme) component of the conjugation machinery. It is needless to say that an intact KPC1 from which the seven–amino acid stretch was deleted could not bind p105 (Fig. 1*B*). We have shown again that the ankyrin repeat domain of p105 mediates its binding to KPC1 (13), thus completing—though indirectly—the identification of the binding domains on both the substrate and its ligase.

An important question was how robust is the WILVRLW binding domain. To study this question, we fused a series of permutations in the sequence to the last 60 amino acids of KPC1 (peptide-KPC1Δ1–1253-FLAG; Fig. 1 *C*, *i*). Association between p105 and KPC1 was observed only with the seven–amino acid–containing KPC1 construct WILVRLW-KPC1Δ1–1253 (Fig. 1*C*). The results strongly suggest that the flanking two tryptophan moieties in the sequence are crucial for the interaction, though later results showed that they are indeed essential but do not have to be on the two termini of the peptide.

**Amino Acid Sequence WILVRLW in KPC1 Is Essential for Ubiquitination of p105.** At that point it was important to show that the binding of p105 to KPC1 via the WILVRLW sequence results in p105's ubiquitination. As is clearly shown in Fig. 2 *A*, *i*, KPC1Δ1–967 ubiquitinates p105 in a dose-dependent manner in a cell-free system. In contrast, the truncated species KPC1Δ1–974 which lacks WILVRLW is inactive. In addition, we checked whether the location of the seven–amino acid sequence in KPC1 is crucial for the conjugating activity. Toward this end, we generated two truncated species of KPC1, WILVRLW-KPC1Δ1–1039 (shown in Fig. 1*A*) and WILVRLW-KPC1Δ1–1061. The two "chimeric" KPCs ubiquitinated p105 in a cell-free system (Fig. 2 *A*, *ii*).

To further confirm that the interaction and the ability to catalyze ubiquitination of p105 depend on its binding to WILVRLW, we tested the ability of isolated peptides, WILVRLW, the N-terminal Trp-deleted peptide ILVRLW, and a scrambled peptide, RIWVWLL, to inhibit conjugation of p105 in a cell-free system, presumably via their ability to compete on the binding of p105 to the ligase. As can be seen in Fig. 2*B*, the scrambled peptide was the most efficient competitor (lanes 9 to 11), followed by the WT one (lanes 6 to 8). The Trp-deleted peptide did not have any competitive activity (lanes 3 to 5).

**Overexpression of Truncated Species of KPC1 that Contain WILVRLW or RIWVWLL Attracts Leukocytes into a Xenograft Tumor Model and Inhibits Tumor Growth.** Since KPC1 and its product p50 exert strong tumor-suppressive activity mediated via multiple mechanisms (13, 14), it was important to examine whether the truncated species of KPC1 that binds to p105 and can conjugate p105 (WILVRLW-KPC1Δ1–1039-FLAG; Fig. 1 *A*, *i*, construct 7, and Fig. 2 *A*, *ii*, lane 4) can also suppress tumor growth in a xenograft tumor model in mice. In addition, since the scrambled peptide RIWVWLL showed a strong inhibitory effect on conjugation of p105 by KPC1 (Fig. 2*B*, lanes 9 to 11), we also decided to examine the suppressive effect of a truncated species of KPC1 that contains the scrambled sequence (RIWVWLL-KPC1Δ1–1039-FLAG). As can be seen in Fig. 3*A*, the two truncated species had a strong suppressive effect on growth of U87-MG–derived xenografts (yellow and gray lines). A truncated KPC1 species that does not contain any derivative of the seven–amino acid p105-binding site did not display a tumor-suppressive effect (Fig. 3*A*,

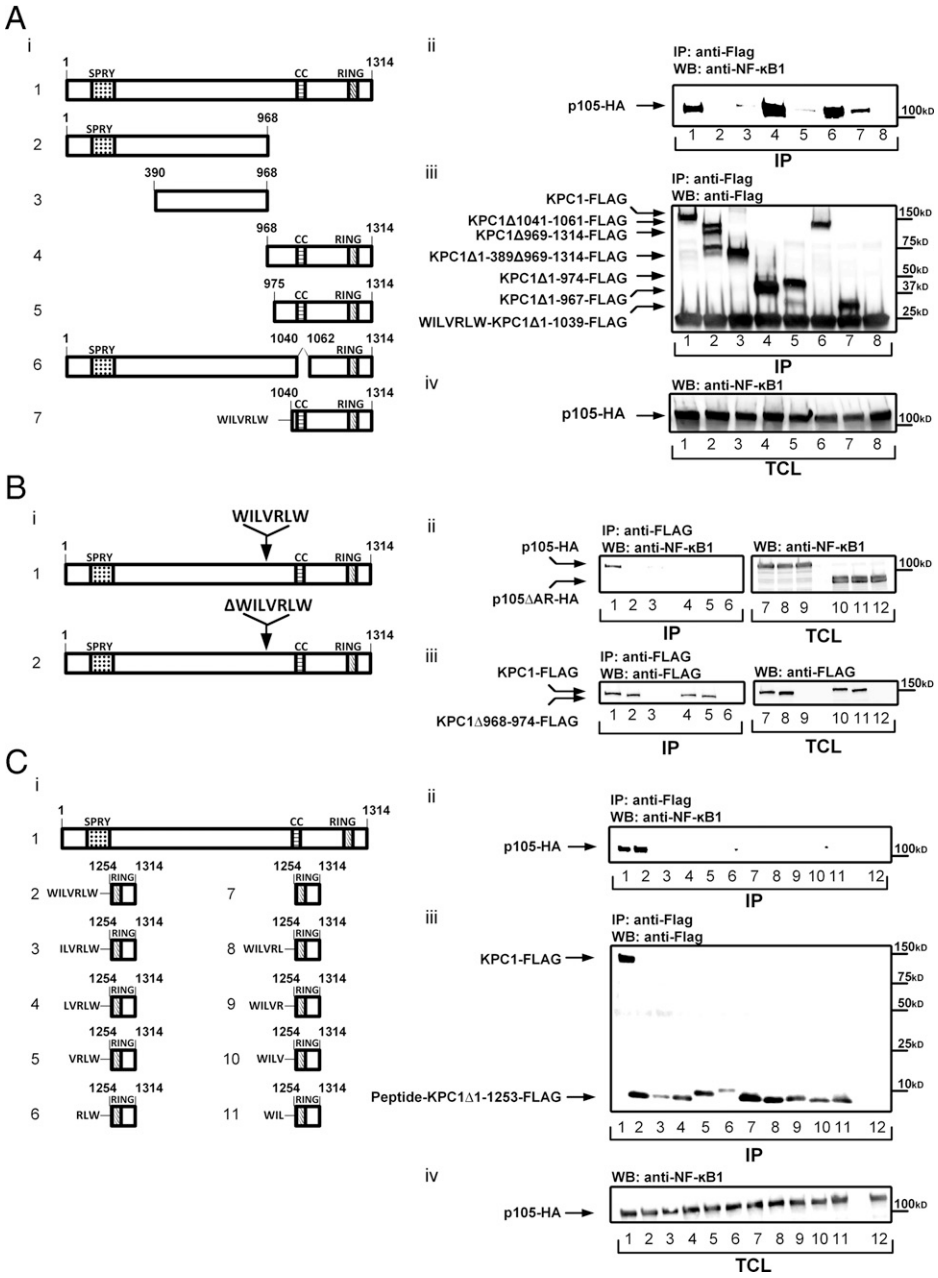


**Fig. 1.** KPC1 interaction with NF-κB1 p105 is mediated via the amino acid stretch WILVRLW (968 to 974) of the ligase. (*A*) Truncated species of KPC1 that lack the amino acid sequence WILVRLW are unable to bind p105. (*A*, *i*) Schematic representation of the KPC1 species used in the experiment shown in *A*, *ii–iv*. (*A*, *ii–iv*) HEK293 cells were transfected with cDNAs coding for p105-HA (lanes 1 to 8), along with different KPC1 species (lanes 1 to 7 correspond to the different KPC1 species depicted in *A*, *i*). Lanes 8 denote extracts from cells that were transfected with an empty vector instead of KPC1. The different KPC1-FLAG species were immunoprecipitated from the total cell lysate (TCL) by immobilized anti-FLAG (*A*, *ii* and *iii*). Proteins were resolved via SDS-PAGE and transferred to a nitrocellulose membrane. p105 was visualized using anti–NF-κB1 (*A*, *ii* and *iv*), and KPC1 species were detected using anti-FLAG (*A*, *iii*). Ten percent of the TCL was analyzed for the expression of the proteins. (*B*) Elimination of the amino acid stretch WILVRLW from KPC1 or the ankyrin repeats (ARs) from p105 results in abrogation of the binding between KPC1 and p105. (*B*, *i*) Schematic representation of the KPC1 species used in the experiment shown in *B*, *ii* and *iii*. (*B*, *ii* and *iii*) HEK293 cells were transfected with cDNAs encoding for p105-HA (lanes 1 to 3) or with cDNAs coding for p105ΔAR-HA (lanes 4 to 6), along with KPC1-FLAG (lanes 1 and 4), KPC1Δ968–974-FLAG (lanes 2 and 5), or an empty vector (lanes 3 and 6). (*B*, *ii*) Visualization of p105-HA and p105ΔAR-HA. (*B*, *iii*) Visualization of the WT and KPC1ΔWILVRLW-FLAG (KPC1Δ968–974-FLAG). Lanes 7 to 9 in *B*, *ii* display WT p105 whereas lanes 10 to 12 display p105ΔAR. Lanes 7 and 8 in *B*, *iii* display WT KPC1 whereas lanes 10 and 11 display the seven–amino acid–depleted KPC1. Lanes 9 and 12 represent cells that were transfected with an empty vector (no KPC1). Immunoprecipitation and visualization of the two different species of KPC1-FLAG and Western blotting of the two different species of p105 were carried out as described for *A*, *ii–iv*. (*C*) The Trp residues in WILVRLW are essential for the binding of KPC1 to p105. (*C*, *i*) Schematic representation of the KPC1 species used in the experiment shown in *C*, *ii–iv*. (*C*, *ii–iv*) HEK293 cells were transfected with cDNAs encoding for p105-HA (lanes 1 to 12), along with the different KPC1 species (lane numbers correspond to the different KPC1 species depicted in *C*, *i*). Lanes 12 denote extracts from cells that were transfected with an empty vector. Peptide-KPC1Δ1–1253-FLAG in *C*, *iii* represents KPC1Δ1–1253-FLAG constructs to which the different WILVRLW derivatives were fused to its N-terminal residue (*C*, *i*). Immunoprecipitation and visualization of the different species of KPC1-FLAG and Western blotting of p105 were carried out as described for *A*, *ii–iv*. IP, immunoprecipitation; WB, Western blotting.

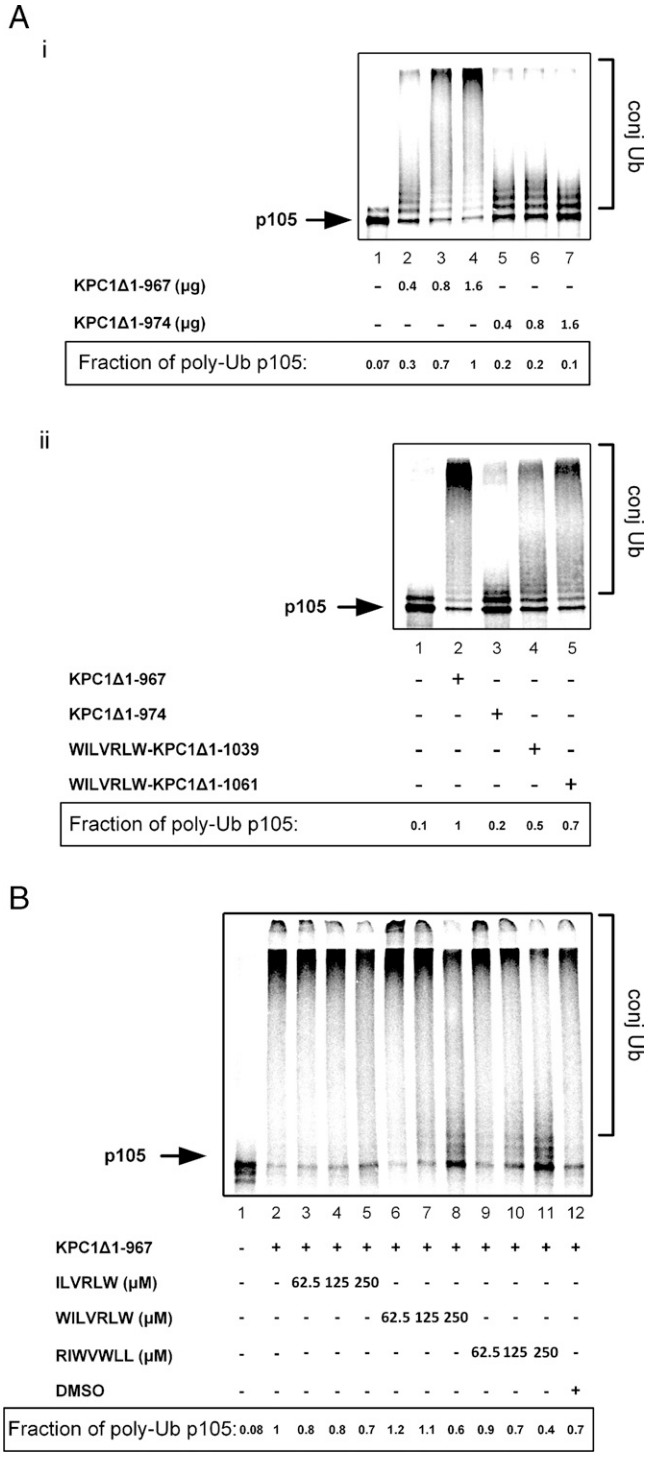


**Fig. 2.** Ubiquitination of p105 by KPC1 is dependent on the amino acid sequence WILVRLW in KPC1. (*A*) In vitro translated $^{35}$S-labeled p105 was ubiquitinated by the indicated purified species of KPC1 in a reconstituted cell-free system as described in *Materials and Methods*. (*A*, *i*) Ubiquitination of p105 by KPC1Δ1–967-His×6 (lanes 2 to 4) and KPC1Δ1–973-His×6 (lanes 5 to 7). The fraction of poly-Ub p105 for each condition is presented (relative to the maximal conjugation; lane 4; arbitrarily designated as 1). (*A*, *ii*) Ubiquitination of p105 using the following species of KPC1: KPC1Δ1–967 (lane 2); KPC1Δ1–974 (lane 3); WILVRLW-KPC1Δ1–1039 (lane 4); and WILVRLW-KPC1Δ1–1061 (lane 5). Each enzyme was added at 0.5 μg. The fraction of poly-Ub p105 was calculated as for *A*, *i* above, but in comparison with lane 2. (*B*) Addition of either the WILVRLW or RIWVWLL peptide inhibits ubiquitination of p105 by KPC1Δ1–967 in a dose-dependent manner. In vitro translated and $^{35}$S-labeled p105 was ubiquitinated by purified KPC1Δ1–967 (lanes 2 to 12) in a cell-free system in the presence of the indicated peptides derived from KPC1: ILVRLW (lanes 3 to 5); WILVRLW (lanes 6 to 8); and RIWVWLL (lanes 9 to 11). The numbers indicate the peptide concentration (μM). Visualization of p105 and its conjugates was carried out using PhosphorImaging. The fraction of poly-Ub p105 for each condition was calculated as described for *A*, *i* above, relative to the conjugates in lane 2.

green line). Of note is that despite the strongest competitive ability of the scrambled peptide on p105 conjugation (Fig. 2*B*), its tumor-suppressive effect was weaker than that of the WT sequence-containing truncated KPC1 (Fig. 3*A*). In correlation with the tumor-suppressive activity of WILVRLW-KPC1Δ1–1039 and RIWVWLL-KPC1Δ1–1039, and in contrast to the lack of effect of KPC1Δ1–1039, the two species also attracted leukocytes to the tumors (Fig. 3*B*) which explains, at least partially, their suppressive effect.

**Proteomic Analysis of Glioblastoma Xenografts Overexpressing Either WT or WILVRLW-KPC1Δ1–1039 Revealed Alterations in Proteins Involved in Biological Pathways That Modulate Malignancies.** In order to examine whether WT KPC1 and its truncated species that lack most of the sequence of the enzyme—but contain either the WT binding domain (WILVRLW) or the scrambled one (RIWVWLL)—elicit similar alterations in the protein profile of the cells in which they are expressed, we analyzed the proteome of the tumors shown in Fig. 3 by mass spectrometry. The reason was that the deleted part of the enzyme might affect cellular processes that are not affected by the deleted species. Surprisingly, we found a strong similarity between tumors overexpressing the WT KPC1 or the truncated species WILVRLW-KPC1Δ1–1039 (Fig. 4). Overexpression of the enzyme that contains RIWVWLL displayed a weaker similarity, possibly explaining the weaker tumor-suppressive activity of this ligase (Fig. 3*A*). Expression of a KPC1 species that lacks altogether the binding site (KPC1Δ1–1039) displayed a proteome that was almost identical to that displayed by expression of an empty vector (Fig. 4). Functional analysis of proteins that were up-regulated significantly in WT KPC1- and WILVRLW-KPC1Δ1–1039–expressing tumors (compared with empty vector–expressing tumors; $P < 0.05$) revealed significant enrichment in proteins involved in cell migration, the extracellular matrix (ECM), cell adhesion, and immune system processes (Fig. 4*B*). Down-regulated proteins highlighted metabolic processes, the cell cycle, and DNA metabolic processes. The mild reduction in cell-cycle proteins in KPC1Δ1–1039 and RIWVWLL-KPC1Δ1–1039 (the number of proteins changed is 15 and 21, respectively) was much smaller than those changed in WT KPC1- and WILVRLW-KPC1Δ1–1039–expressing tumors (80 and 120, respectively). The raw data of the up- and down-regulated proteins are enclosed as a separate file (Dataset S1).

**WILVRLW- and RIWVWLL-pVHL Ligand-Based PROTACs Induce Ubiquitination of p105 by the E3 Ub Ligase pVHL in a Reconstituted Cell-Free System.** Identification of a short and defined site in KPC1 that binds p105 paved the way for design of a PROTAC that would supposedly target p105 for processing. If successful, such PROTACs can serve as a base for the development of a novel tumor-suppressive drug. Thus, we synthesized a series of PROTACs that are based on the WILVRLW binding peptide and are connected via a linker to the pVHL ligand (Fig. 5*A* and *SI Appendix*, Figs. S1 and S2).

As can be seen in Fig. 5 *B*, *i*, the WILVRLW-SG-PEG-pVHL-ligand PROTAC stimulates ubiquitination of p105 in a dose-dependent manner. Interestingly, the RIWVWLL-SG-PEG-pVHL-ligand PROTAC stimulates ubiquitination of p105 even more (Fig. 5 *B*, *ii*, compare lanes 8 and 9; see also

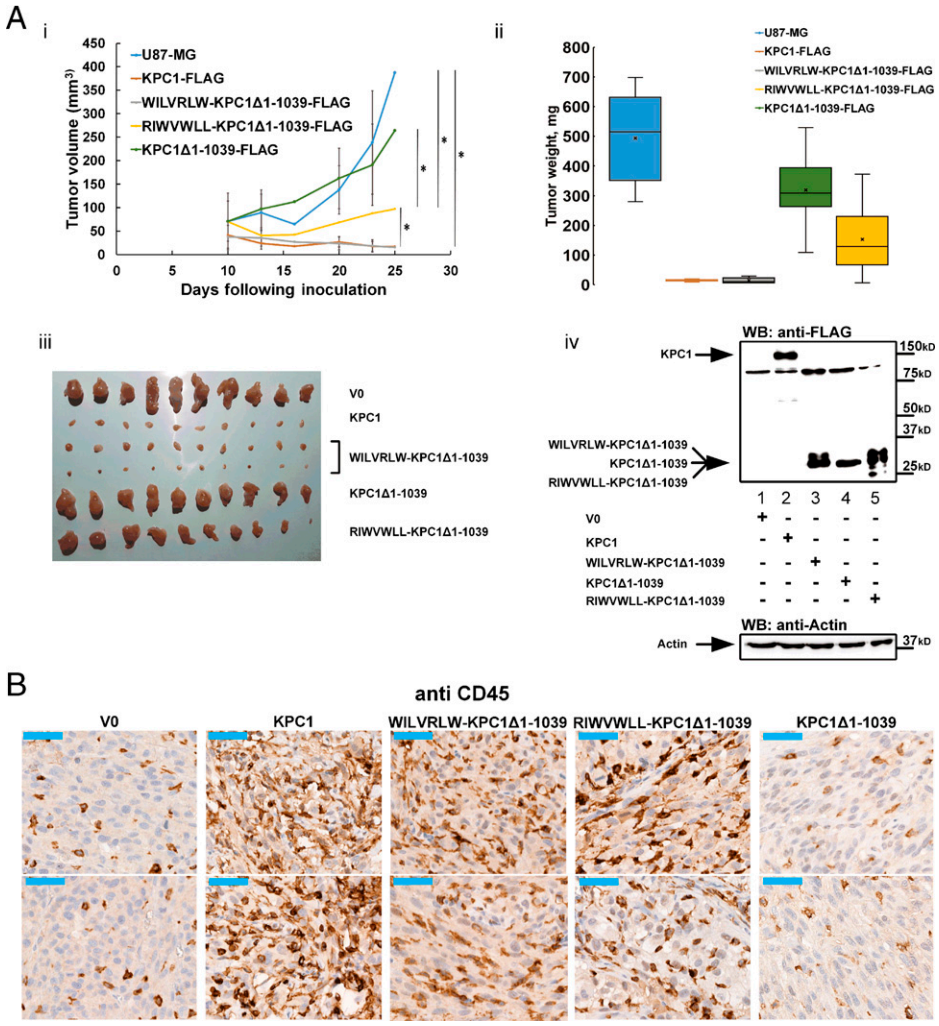


**Fig. 3.** Overexpression of truncated species of KPC1 that contain the amino acid sequence WILVRLW or RIWVWLL attracts leukocytes into a xenograft tumor model and inhibits tumor growth. (*A*, *i* and *ii*) Growth rates (*$P < 0.05$) (*i*) and weights (at the end of the experiment, 25 d after inoculation) (*ii*) of U87-MG cell–derived xenografts grown in severe combined immunodeficiency (SCID) mice. The tumors express either KPC1-FLAG, WILVRLW-KPC1Δ1–1039-FLAG, RIWVWLL-KPC1Δ1–1039-FLAG, or KPC1Δ1–1039-FLAG proteins. Control cells were transfected with an empty vector. (*A*, *iii*) Tumors derived from U87-MG cells at the end of the experiment. (*A*, *iv*) The different species of KPC1 stably expressed in the U87-MG cells used in the experiment. Western blotting of extracts derived from the different cells was carried out using an anti-FLAG antibody as described for Fig. 1. (*B*) Tumor sections expressing the indicated KPC1 species attract leukocytes as is evident from immunohistochemical staining with anti-CD45. All scale bars (in the upper left corner of each panel), 50 μm.

*Discussion*). An IWVWLL-based PROTAC that contains a SerGly linker was active almost like the WT PROTAC, but removal of the Gly residue from the linker decreased the conjugation activity significantly (Fig. 5 *B*, *ii*, compare lanes 5 and 6) which highlights the importance of the linker in the conjugation-stimulating activity. Also, removal of the two Trp residues weakened the activity significantly, even in the presence of the GlySer linker (Fig. 5 *B*, *ii*, lane 4).

**The Seven–Amino Acid–Based PROTACs Stimulate the Interaction between p105 and pVHL and Enhance the Generation of p50 in Cells, and Consequently Restrict Cell Growth.** After confirming the activity of the PROTACs in a cell-free system, it was important to test their effects in cells. To track the penetration of the PROTACs into cells, we synthesized the RIWVWLLC (-FITC)G-PEG-pVHL-ligand PROTAC which contains the fluorophore fluorescein isothiocyanate (FITC) (Fig. 6 *A*, *i* and *SI Appendix*, Figs. S1 and S2). Using a confocal microscope, we observed that the FITC-labeled PROTAC penetrates into HEK293 cells (Fig. 6 *A*, *ii*) and can stimulate p105 conjugation in a cell-free system (*SI Appendix*, Fig. S3).

In a coimmunoprecipitation experiment in HEK293 cells, we found that the interaction between p105 and pVHL was negligible in the absence of PROTACs but increased significantly following the addition of either WILVRLW- or RIWVWLL-based PROTACs (Fig. 6 *B*, *i*). Importantly, the two PROTACs stimulated in cells the formation of p50 from the expressed p105 (Fig. 6*C*).

Last, we checked for the PROTACs' ability to restrict the growth of U87-MG cells. We added the RIWVWLL- and WILVRLW-based PROTACs to the growth medium of the cells (as described in *Materials and Methods*) and tracked their growth for 3 d. At all measuring points, the PROTACs inhibited the growth rate of the cells (in a statistically significant manner) compared with dimethyl sulfoxide (DMSO)–treated cells (Fig. 6*D*).

## Discussion

We have previously shown that the Ub ligase KPC1 conjugates Ub to p105, the NF-κB long precursor, resulting in its limited proteasomal processing to the p50 active subunit of the mature transcriptional regulator (13). Furthermore, we have shown

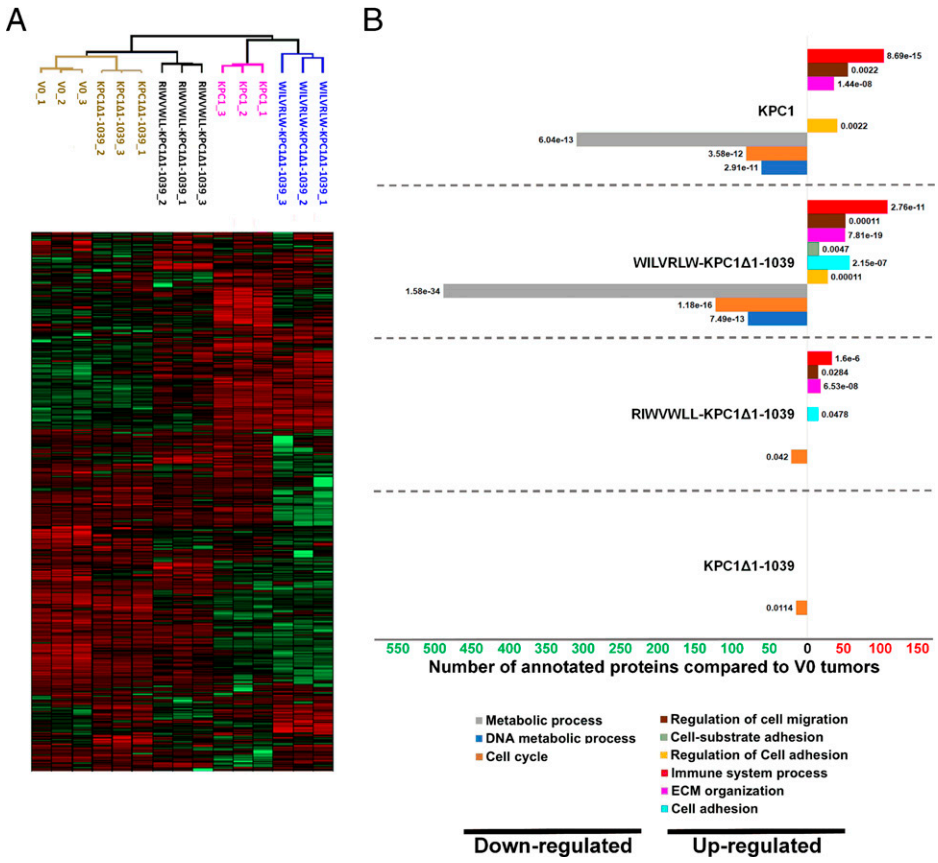


**Fig. 4.** Proteome analysis of glioblastoma xenografts expressing different species of KPC1. (*A*) Euclidean heatmap diagram presenting an unsupervised hierarchical clustering of the cellular proteome under expression of the different KPC1 species. The clustering was based on the intensities of the identified proteins (low intensity, green; high intensity, red), and was generated by Perseus software. (*B*) Functional analysis of proteins that are up- (red) or down- (green) regulated (compared with tumors transfected with an empty vector with $P < 0.05$). Shown are selected annotation clusters with false discovery rate (FDR) <0.05 (the numbers on the flanks of each column represent the FDR of the indicated cluster). Functional analysis was carried out using String software (https://string-db.org/). Proteome analysis was carried out on the xenografts described for Fig. 3. The raw proteomic data are in Dataset S1.

that the excess of p50 which results from overexpression of KPC1 exerts a strong tumor-suppressive effect mediated by several mechanisms, mostly related to recruitment of the immune system (14). In the current study, we identified the domain in KPC1 to which p105 binds, and found that it is an exceptionally short, seven–amino acid stretch that spans residues 968 to 974 in the KPC1 sequence (WILVRLW). A synthetic peptide that spans this sequence inhibited KPC1-mediated conjugation of Ub to p105 (Fig. 2*B*). A truncated species of the enzyme that lacks the major part of the protein (1,039 amino acids out of 1,314 residues) but contains the RING-finger domain necessary for binding the E2 component of the conjugation machinery and the seven–amino acid–binding domain can conjugate Ub to p105 (Fig. 2 *A*, *ii*), suppress tumor growth (Fig. 3*A*), and attract leukocytes to the tumor (Fig. 3*B*). Proteomic analysis revealed that the seven–amino acid–binding domain–containing short KPC1 species altered the expression of several sets of proteins related to tumorigenesis in a similar way induced by WT KPC1 (Fig. 4). An interesting question related to the ability of the truncated enzyme to catalyze conjugation of p105 is why such a long protein is necessary at all. One answer is that p105 is not the only substrate of the ligase, and other substrates such as p27 (15) are recognized by different domains.

Based on this information, we decided to synthesize a PROTAC that contains the binding sequence, with the hope that it would generate an excess of p50 and serve as a prototype for a tumor-suppressive modality.

Out of the myriad UPS substrates, p105 is a rare example that undergoes both a complete degradation and limited processing, mediated by different ubiquitin ligases and signaling mechanisms. A unique long Gly-Ala repeat in the middle of the p105 sequence was characterized as a "stop" proteasomal signal that—once encountered by the proteasome—results in release of the p50 active subunit which is the N-terminal part of the p105 precursor (20, 21). With this information at hand, we assumed that substitution of the natural ligase KPC1 by an artificially recruited VHL complex would faithfully imitate ubiquitination and subsequent limited processing of p105 to p50. An as-yet unsolved enigma is the switch that modulates processing and complete destruction. Indeed, the PROTAC stimulated conjugation of Ub to p105 in a reconstituted cell-free system (Fig. 5*B*) and processing of p105 to p50 in cells. Further, it restricted cell growth when added to the growth medium.

When attempting to optimize the binding sequence and identify critical residues within it, we noted a discrepancy between the activity of a scrambled peptide (RIWVWLL) in a cell-free system and in cells/tumors. Thus, the peptide was a slightly better competitor than its WT counterpart (WILVRLW) in a cell-free reconstituted conjugation system (Fig. 2*B*). Also, when it was part of a PROTAC, it stimulated conjugation of Ub to p105 more efficiently than the WT peptide-based PROTAC (Fig. 5 *B*, *ii*). Yet, when the scrambled peptide (now fused to truncated KPC1) was tested for its ability to suppress tumors (Fig. 3) or to alter the cellular proteome to display a "tumor-suppressive" landscape (Fig. 4),

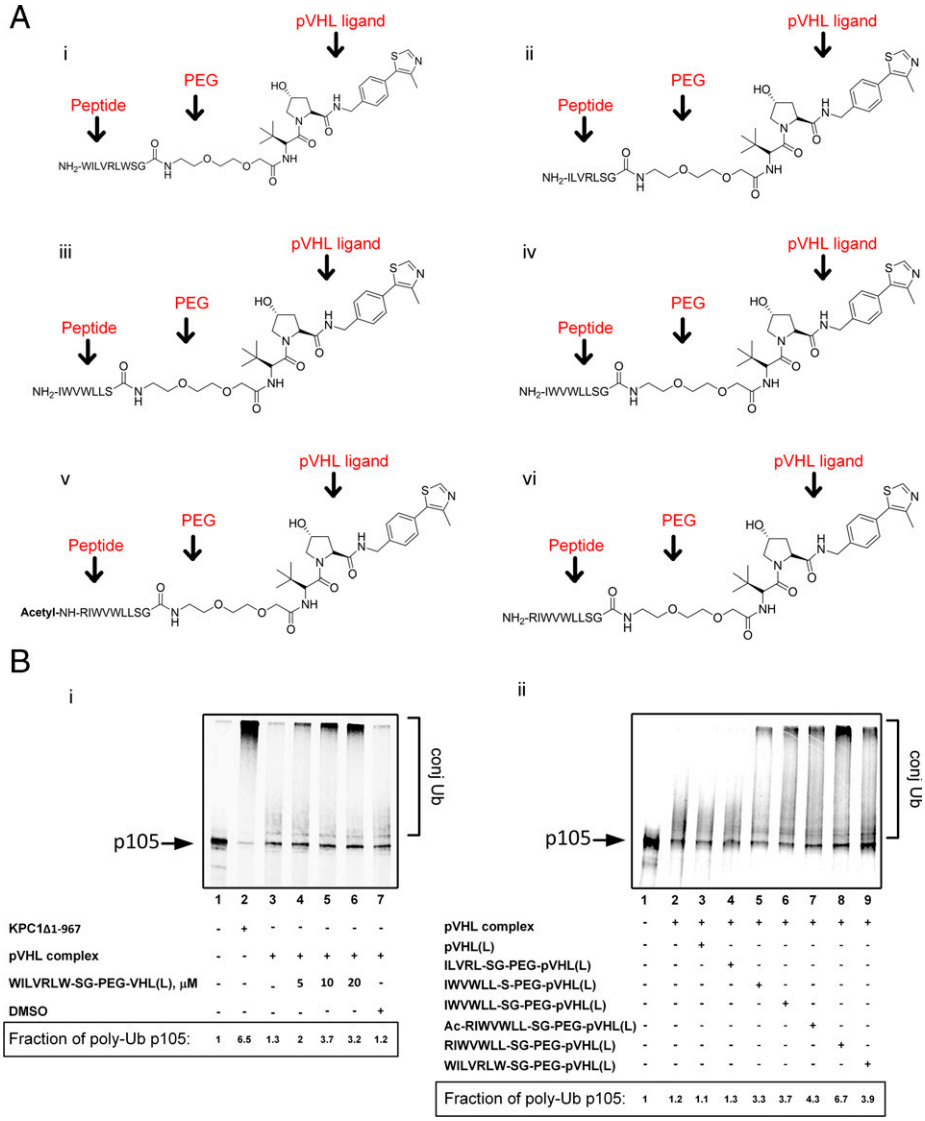


**Fig. 5.** PROTACs containing the peptide WILVRLW or RIWVWLL induce ubiquitination of p105 by the E3 ligase pVHL in a reconstituted cell-free system. (*A*) Schematic structure of the different PROTACs. (*B*) In vitro translated and $^{35}$S-labeled p105 is ubiquitinated in a cell-free system by purified pVHL complex mediated by PROTACs that contain the KPC-binding site or some of its derivatives. (*B*, *i*) Ubiquitination of p105 by KPC1Δ1–967 (lane 2) or by purified pVHL complex (lanes 3 to 7) mediated by the WILVRLWSG-PEG-pVHL(L) ligand PROTAC (lanes 4 to 6). The numbers indicate the PROTAC concentration (μM). (*B*, *ii*) Similar to the experiment depicted for *B*, *i* but with the different indicated PROTACs (20 μM each). The fraction of poly-Ub p105 for each condition was calculated as described in the legend for Fig. 2 *A*, *i* in comparison with lane 1. Proteins were visualized using PhosphorImaging. (L), ligand.

the WT peptide was superior. The possible explanation of the discrepancy between the WT and scrambled peptides might reside in the position of the two tryptophans. As is shown in Fig. 2*B* (lanes 3 to 5), a peptide that lacks only one tryptophan does not inhibit ubiquitination of p105 by purified KPC1, compared with its intact counterpart (lanes 6 to 8) or a scrambled peptide (lanes 9 to 11). Similarly, in Fig. 5 *B*, *ii* (lane 4), we show that a PROTAC molecule that has five amino acids and lacks both tryptophans cannot "glue" the VHL complex to p105, and therefore does not stimulate its ubiquitination. It is possible that the distance between the two tryptophan residues plays an essential role in the strength of the interaction between p105 and KPC1. In the scrambled sequence, the two tryptophans reside in closer vicinity, probably resulting in increased binding affinity. Nevertheless, as noted, the miniligase containing the scrambled peptide was less efficient in tumor suppression in the xenograft model, which might be due to a higher sensitivity to aminopeptidases. Further optimization of the binding sequence might require better understanding of the structure of p105 along with the different peptides, and might need to go hand-in-hand with stabilization of the PROTAC (see above and below).

Disappointingly, we could not observe a tumor-suppressive activity of the PROTAC. This might be due to the required long-term treatment and lack of stability of the PROTAC over time. We assume that the peptide-based PROTAC is sensitive to proteolysis in the tumor cells, the tumor's microenvironment, and the circulation and normal mouse tissues of the host, and that its distribution in the body did not allow build-up of a high enough concentration in the tumor to affect its growth. Stabilization will require further optimization of the PROTAC, though we have clearly shown a proof of concept for a recognition site–based PROTAC. Several approaches can be attempted in order to render it more stable, among them 1) backbone cyclization; 2) use of D-amino acids; and 3) screening for small molecules that bind p105 similar to the seven amino acids that will then substitute for the peptide in the PROTAC. It should

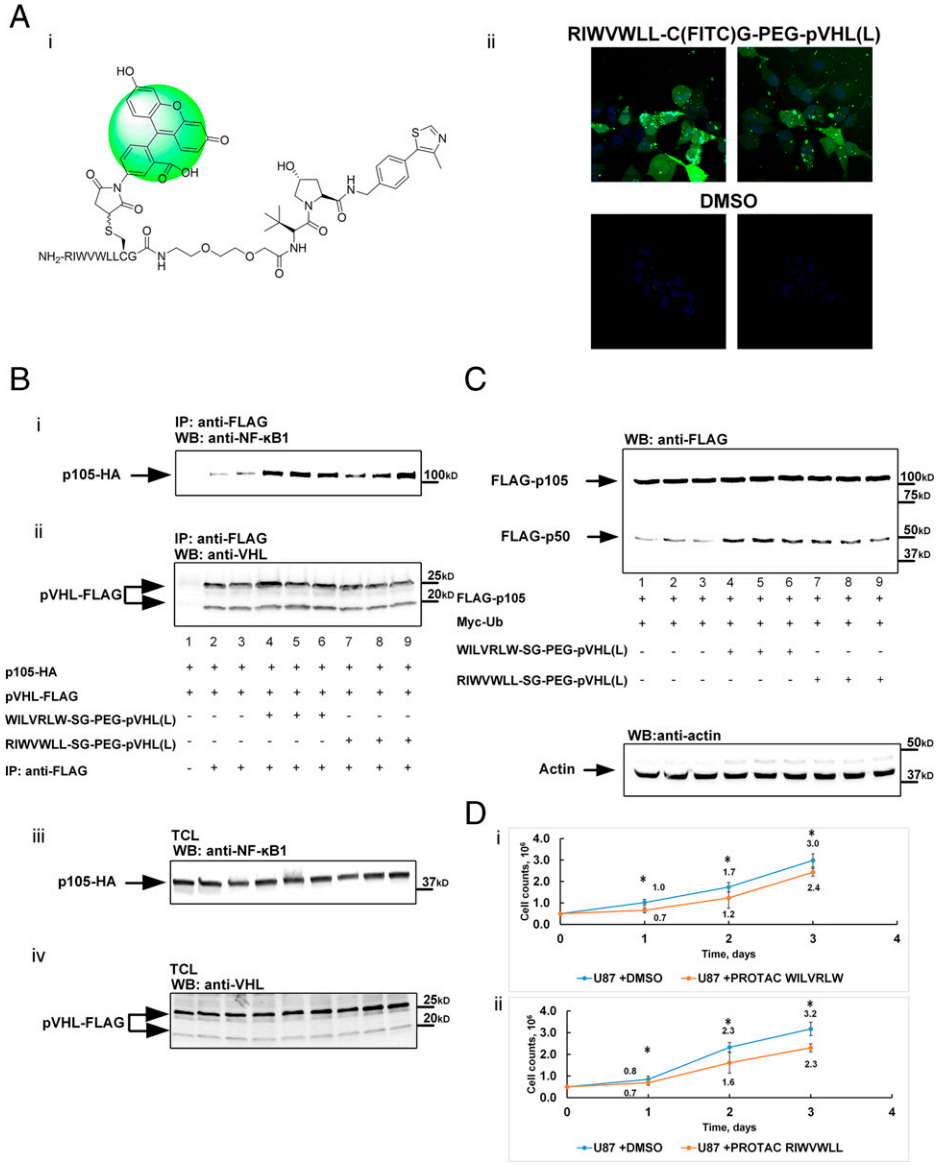


**Fig. 6.** PROTACs that contain the WILVRLW or RIWVWLL peptide stimulate interaction between p105 and pVHL and subsequent processing of p105 to p50, and restrict cell growth. (*A*) The PROTAC RIWVWLL-C(-FITC)G-PEG-pVHL(L) is cell-permeable. (*A*, *i*) Schematic representation of the PROTAC RIWVWLL-C(-FITC)G-PEG-pVHL(L). (*A*, *ii*) Confocal microscopy imaging of HEK293 cells 24 h after addition of the RIWVWLL-C(FITC)G-PEG-pVHL-ligand PROTAC to the growth medium (25 μM). (*B*) The interaction between p105 and pVHL in cells is stimulated by WILVRLW- or RIWVWLL-based PROTACs (25 μM). HEK293 cells that stably express pVHL-FLAG were transfected with p105-HA (lanes 1 to 9). pVHL-FLAG was immunoprecipitated from the cell lysate using immobilized anti-FLAG. p105-HA (*B*, *i*) and pVHL-FLAG (*B*, *ii*) were visualized using the appropriate antibodies as indicated. *B*, *iii* and *iv* display the two proteins in the TCL. (*C*) WILVRLW- and RIWVWLL-based PROTACs enhance cellular processing of p105 to p50. HEK293 cells that stably express pVHL-FLAG were transfected with cDNAs coding for FLAG-p105 along with Myc-Ub. WILVRLW- or RIWVWLL-based PROTACs (25 μM) were added to the growth medium as indicated. FLAG-p105 and FLAG-p50 were visualized using an anti-FLAG antibody. Actin was used as a loading control. (*D*) WILVRLW- or RIWVWLL-based PROTACs restrict growth of U87-MG cells. (*D*, *i*) Growth curve of U87-MG cells in the presence of the WILVRLWSG-PEG-pVHL(L) PROTAC (25 μM). (*D*, *ii*) Similar to *D*, *i*, but in the presence of the RIWVWLLSG-PEG-pVHL(L) PROTAC. *$P < 0.05$.

be noted that peptide-based PROTACs are being tested these days for a variety of pathologies, for example a PROTAC that aims to target the estrogen receptor (22).

## Materials and Methods

**Materials.** Materials for sodium dodecyl sulfate–polyacrylamide gel electrophoresis (SDS-PAGE), Bradford assay, and enhanced chemiluminescence were from Bio-Rad. Molecular mass markers and L-[$^{35}$S]methionine were from GE Healthcare. Tissue-culture media, sera, and supplements for growing HEK293 (ATCC CRL1573) and U87-MG (ATCC HTB14) cells were from Biological Industries. Formalin solution for histological tissue fixation was from Sigma. Immobilized mouse anti-FLAG (M2), mouse anti-FLAG (M2), and rabbit anti–NF-κB1 were from Sigma. Rabbit anti–Von Hippel–Lindau (VHL) antibody (ab83307) and rabbit anti-CD45 (ab10558) were from Abcam. Mouse anti-actin was from Millipore. Peroxidase-conjugated secondary antibody was from Jackson ImmunoResearch Laboratories. Immunohistochemistry staining was carried out using the iVIEW DAB Detection Kit from Ventana Medical Systems. jetOPTIMUS DNA transfection reagent was from Polyplus-transfection. Hepes and Tris buffers, adenosine 5′-[γ-thio]triphosphate (ATPγS), dithiothreitol (DTT), Ub-activating enzyme (E1), and Ub were from Sigma. Protease inhibitor mixture was from Roche. Ub aldehyde (UbAl) was from Biomol. The TNT T7 Quick Coupled Transcription/Translation System was from Promega. Synthesis of KPC1-derived peptides was carried out by Bio Basic. Recombinant human VHL–ELOB–ELOC–CUL2–RBX1 complex was

from R&D Systems. Restriction and modifying enzymes were from New England Biolabs. Oligonucleotides were from Syntezza Bioscience. C.B-17/IcrHsd-Prkdc$^{scid}$ mice were from Envigo.

**Methods.**

***Plasmids.*** cDNA coding for FLAG-p105 and 6×HIS-Ubc5c (13) and for Myc-Ub (23) is described in the indicated references. For transient transfection in cells, the following cDNAs coding for truncated species of KPC1-FLAG were cloned into the pCAGGS 3.2 FLAG expression vector: KPC1Δ1041–1061 and KPC1Δ968–974 (amplified using primers containing the restriction sites EcoRI and NotI); KPC1Δ969–1314 and KPC1Δ1–973 (amplified using primers containing the restriction sites BamHI and XhoI); KPC1Δ1–967 and WILVRLW-KPC1Δ1–1039 (amplified using primers containing the restriction sites NdeI and XhoI or BamHI and NotI, respectively); KPC1; KPC1Δ1–389;Δ696–1314; WILVRLW-KPC1Δ1–1253; ILVRLW-KPC1Δ1–1253; LVRLW-KPC1Δ1–1253; VRLW-KPC1Δ1–1253; RLW-KPC1Δ1–1253; KPC1Δ1–1253; WILVRL-KPC1Δ1–1253; WILVR-KPC1Δ1–1253; WILV-KPC1Δ1–1253; and WIL-KPC1Δ1–1253 (amplified using primers containing the restriction sites EcoRI and XhoI). cDNA coding for p105-HA was cloned into the CMV-5-B expression vector (amplified using primers containing the restriction sites NotI and KpnI).

For protein expression in bacteria, the following cDNAs, coding for truncated species of KPC1, were cloned into the pT7b-6×HIS expression vector: KPC1Δ1–967; KPC1Δ1–974; WILVRLW-KPC1Δ1–1039; and WILVRLW-KPC1Δ1–1061 (all amplified using primers containing the restriction sites NdeI and HindIII).

For stable expression in cells, the following cDNAs were cloned into the NSPI-CMV MCS lentiviral expression vector: WILVRLW-KPC1Δ1–1039; KPC1Δ1–1039; and RIWVWLL-KPC1Δ1–1039 (amplified using primers containing the restriction site XhoI); KPC1-FLAG; and pVHL-FLAG (amplified using primers containing the restriction sites BamHI and XhoI).

***Cell culture.*** U87-MG and HEK293 cells were grown at 37 °C and 5% $CO_2$ in Dulbecco's modified Eagle's medium supplemented with penicillin-streptomycin and 10% fetal calf serum.

***Stable expression.*** Stable expression of cDNAs coding for KPC1, WILVRLW-KPC1Δ1–1039, KPC1Δ1–1039, RIWVWLL-KPC1Δ1–1039, and pVHL-FLAG in U87-MG and HEK293 cell lines was carried out as described previously (13). Cells stably expressing the above proteins were selected by puromycin (U87-MG, 5 μg/mL; HEK293, 2 μg/mL).

***Interaction between p105 and KPC1 species.*** For analysis of the interaction between p105 and KPC1 species, HEK293 cells were transfected with various cDNAs coding for WT and the truncated species of KPC1-FLAG, or with an empty vector along with p105-HA. The transfection was carried out using the jetOPTIMUS transfection reagent. After 48 h, cells were lysed with RIPA buffer (150 mM NaCl, 50 mM Tris·HCl, pH 8.0, 0.5% sodium deoxycholate, 1% Nonidet P-40, 0.1% SDS, and freshly added protease inhibitor mixture). Lysates were incubated with immobilized anti-FLAG at 4 °C for 2 h. At the end of the incubation, the beads were washed five times with RIPA buffer. Proteins were resolved by SDS-PAGE and visualization of the coimmunoprecipitated p105-HA was carried out using an anti–NF-κB1 antibody.

***Expression of proteins in bacteria.*** cDNAs coding for KPC1Δ1–967-HIS×6, KPC1Δ1–974-HIS×6, WILVRLW-KPC1Δ1–1039-HIS×6, and WILVRLW-KPC1Δ1–1061-HIS×6 (in pT7b-6×HIS) were transfected into pLysS *Escherichia coli* competent cells [Rosetta(DE3)pLysS; Novagen]. The pLysS bacteria were grown at 37 °C and brought to an optical density (O.D.) of 0.7. Protein expression was induced by isopropyl β-D-1-thiogalactopyranoside (IPTG; 500 μM). Four hours after induction, cells were lysed by sonication in a buffer containing 0.1 M NaCl, 20 mM Tris·HCl (pH 7.6), 10 mM β-mercaptoethanol, and ethylenediaminetetra-acetate (EDTA)-free protease inhibitor mixture.

***In vitro translation.*** In vitro translation of L-[$^{35}$S]methionine–labeled p105 was carried out using the TnT Quick Coupled Transcription/Translation System according to the manufacturer's protocols.

***Ub conjugation to p105 in a cell-free system.*** In vitro translated and $^{35}$S-labeled NF-κB1 p105 was ubiquitinated in a 12.5-μL reaction mixture that contained Ub (0.5 μg), E1 (0.25 μg), 6×His-Ubc5c (0.75 μg), UbAl (0.5 μg), ATPγS (2 mM), and one of the following E3 ligases: KPC1Δ1–967-HIS×6 (0.5 μg or as indicated), KPC1Δ1–974-HIS×6 (0.5 μg or as indicated), WILVRLW-KPC1Δ1–1039-HIS×6 (0.5 μg), WILVRLW-KPC1Δ1–1039-HIS×6 (0.5 μg), or pVHL complex (0.5 μg). The reaction was carried out at 37 °C for 30 min in the presence or absence of KPC1-derived peptides (ILVRLW, WILVRLW, or RIWVWLL) or PROTACs at the indicated concentrations (μM). The conjugation reaction was terminated by the addition of a fivefold-concentrated sample buffer. Proteins were resolved by SDS-PAGE (7.5%) and visualized via PhosphorImaging.

***Tumorigenicity.*** Exponentially growing U87-MG cells that stably express KPC1, WILVRLW-KPC1Δ1–1039, KPC1Δ1–1039, or RIWVWLL-KPC1Δ1–1039 were dissociated by trypsin and brought to a concentration of $60 \times 10^6$ per milliliter in phosphate-buffered saline (PBS). Six- to 10-wk-old C.B-17/IcrHsd-Prkdc$^{scid}$ mice were injected with $6 \times 10^6$ cells (0.1 mL) subcutaneously to each flank (each type of cell was injected into at least five mice). Xenograft size was measured using a caliper. The volume of the tumors was calculated as follows: volume = length × width$^2$ × 0.5. At the end of the experiment, tumors were resected, weighed, and fixed in formalin for 48 h. Animal experiments, protocols, and procedures were approved by the Technion's ethics committee for animal experiments.

***Immunohistochemistry.*** Formalin-fixed xenograft tumors were embedded in paraffin; 5-μm-thick sections were stained by rabbit anti-CD45 (1:3,000) using the Ventana BenchMark ULTRA IHC/ISH System. Visualization was performed by the iVIEW DAB Detection Kit according to the manufacturer's protocols.

***Mass spectrometry analysis of U87-MG–derived tumors.*** After grinding (Omni TH tissue homogenizer) and two rounds of sonication, proteins from frozen xenografts were isolated using a solution containing urea (9 M), ammonium bicarbonate (0.4 M), and DTT (10 mM). Aliquots of 20 μg protein each from the different tumors were treated with DTT (3 mM; at 60 °C for 30 min), and the -SH groups were modified with a solution of iodoacetamide (9 mM) dissolved in ammonium bicarbonate (0.4 M; in the dark at room temperature for 30 min). The proteins were then digested overnight at 37 °C by modified trypsin (Promega; dissolved in a solution of 1 M urea and 50 mM ammonium bicarbonate) at a ratio of 1:50 enzyme to substrate. A second similar amount of trypsin was added for an additional 4 h. Proteomic analysis of the peptides was carried out as described elsewhere (13, 24).

***Synthesis of PROTACs.*** PROTACs were synthesized as described in detail in *SI Appendix* (*SI Appendix, Text* and Figs. S1 and S2).

***PROTAC's cell intake.*** HEK293 cells were seeded on a glass-bottom 35-mm dish and incubated in the presence of either FITC or a FITC-labeled PROTAC (25 μM) for 16 h. After the incubation, the medium was removed and the cells were washed with PBS prior to imaging, which was carried out using a Zeiss LSM 700 confocal microscope.

***PROTACs mediate the interaction between p105 and pVHL.*** For analysis of the interaction between p105 and pVHL ligand-based PROTACs, HEK293 cells that stably express pVHL-FLAG were transfected with cDNAs coding for HA-p105. Twenty-four hours after transfection, the medium was replaced and the PROTACs were added. Cells were then incubated for an additional 16 h and lysed with a buffer containing 150 mM NaCl, 50 mM Tris·HCl (pH 7.5), 0.5% Nonidet P-40, and freshly added protease inhibitor mixture. Lysates were incubated with immobilized anti-FLAG at 4 °C for 2 h. After the incubation, beads were washed five times with the above buffer. Proteins were resolved by SDS-PAGE and visualization of the immunoprecipitated pVHL-FLAG was performed using an anti-FLAG antibody. The coimmunoprecipitated p105-HA was visualized using an anti–NF-κB1 antibody.

***Stimulation of p105 processing by PROTACs in cells.*** HEK293 cells that stably expressed pVHL were transfected with cDNAs coding for FLAG-p105 and Myc-Ub. Twenty-four hours after the transfection, the medium was replaced and the PROTACs were added. Following incubation for 16 h, cells were lysed with RIPA buffer and proteins were resolved by SDS-PAGE. FLAG-p105 and FLAG-p50 were visualized using an anti-FLAG antibody.

***Cell counting.*** U87-MG cells ($0.5 \times 10^6$) were seeded on a 60-mm dish and incubated (for 1 to 3 d) with either the RIWVWLLSG-PEG-pVHL-ligand or the WILVRLWSG-PEG-pVHL-ligand PROTAC (25 μM). On each day, a triplicate of the PROTAC-treated dishes and a triplicate of control dishes were removed, and the cells were dispersed by trypsin and counted using the Beckman Coulter Vi-CELL XR Cell Viability Analyzer.

***Statistical analysis.*** Data in graphs represent the mean ± SD. Experiments were statistically analyzed by the two-tailed *t* test. A *P* value <0.05 was considered statistically significant.

**Data Availability.** All study data are included in the article and/or supporting information.

**ACKNOWLEDGMENTS.** A.C. was supported by grants from the Adelson Medical Research Foundation, the Israel Science Foundation, and the Albert Sweet Foundation. A.C. is an Israel Cancer Research Fund Professor. We thank Dr. Craig M. Crews for his assistance in designing the pVHL ligand-based PROTAC.

1. J. A. DiDonato, F. Mercurio, M. Karin, NF-κB and the link between inflammation and cancer. *Immunol. Rev.* **246**, 379–400 (2012).

2. J. C. Betts, G. J. Nabel, Differential regulation of NF-kappaB2(p100) processing and control by amino-terminal sequences. *Mol. Cell. Biol.* **16**, 6363–6371 (1996).

3. V. J. Palombella, O. J. Rando, A. L. Goldberg, T. Maniatis, The ubiquitin-proteasome pathway is required for processing the NF-κB1 precursor protein and the activation of NF-κB. *Cell* **78**, 773–785 (1994).
4. M. S. Hayden, S. Ghosh, NF-κB, the first quarter-century: Remarkable progress and outstanding questions. *Genes Dev.* **26**, 203–234 (2012).
5. K. Taniguchi, M. Karin, NF-κB, inflammation, immunity and cancer: Coming of age. *Nat. Rev. Immunol.* **18**, 309–324 (2018).
6. Y. Xia, S. Shen, I. M. Verma, NF-κB, an active player in human cancers. *Cancer Immunol. Res.* **2**, 823–830 (2014).
7. W. Weichert *et al.*, High expression of RelA/p65 is associated with activation of nuclear factor-kappaB-dependent signaling in pancreatic cancer and marks a patient population with poor prognosis. *Br. J. Cancer* **97**, 523–530 (2007).
8. S. Shukla *et al.*, Nuclear factor-kappaB/p65 (Rel A) is constitutively activated in human prostate adenocarcinoma and correlates with disease progression. *Neoplasia* **6**, 390–400 (2004).
9. T. Cartwright, N. D. Perkins, C. L Wilson, NFKB1: A suppressor of inflammation, ageing and cancer. *FEBS J.* **283**, 1812–1822 (2016).
10. G. Schneider *et al.*, IKKalpha controls p52/RelB at the skp2 gene promoter to regulate G1- to S-phase progression. *EMBO J.* **25**, 3801–3812 (2006).
11. D. J. Voce *et al.*, Nfkb1 is a haploinsufficient DNA damage-specific tumor suppressor. *Oncogene* **34**, 2807–2813 (2015).
12. O. Tarcic *et al.*, RNF20 links histone H2B ubiquitylation with inflammation and inflammation-associated cancer. *Cell Rep.* **14**, 1462–1476 (2016).
13. Y. Kravtsova-Ivantsiv *et al.*, KPC1-mediated ubiquitination and proteasomal processing of NF-κB1 p105 to p50 restricts tumor growth. *Cell* **161**, 333–347 (2015).
14. Y. Kravtsova-Ivantsiv *et al.*, Excess of the NF-κB p50 subunit generated by the ubiquitin ligase KPC1 suppresses tumors via PD-L1- and chemokines-mediated mechanisms. *Proc. Natl. Acad. Sci. U.S.A.* **117**, 29823–29831 (2020).
15. S. Kotoshiba, T. Kamura, T. Hara, N. Ishida, K. I. Nakayama, Molecular dissection of the interaction between p27 and Kip1 ubiquitylation-promoting complex, the ubiquitin ligase that regulates proteolysis of p27 in G1 phase. *J. Biol. Chem.* **280**, 17694–17700 (2005).
16. Y. Haupt, Y. Barak, M. Oren, Cell type-specific inhibition of p53-mediated apoptosis by mdm2. *EMBO J.* **15**, 1596–1606 (1996).
17. Y. Haupt, R. Maya, A. Kazaz, M. Oren, Mdm2 promotes the rapid degradation of p53. *Nature* **387**, 296–299 (1997).
18. J. Liu *et al.*, PROTACs: A novel strategy for cancer therapy. *Semin. Cancer Biol.* **67**, 171–179 (2020).
19. M. Pettersson, C. M. Crews, PROteolysis TArgeting Chimeras (PROTACs)—Past, present and future. *Drug Discov. Today. Technol.* **31**, 15–27 (2019).
20. A. Orian *et al.*, Structural motifs involved in ubiquitin-mediated processing of the NF-kappaB precursor p105: Roles of the glycine-rich region and a downstream ubiquitination domain. *Mol. Cell. Biol.* **19**, 3664–3673 (1999).
21. L. Lin, S. Ghosh, A glycine-rich region in NF-kappaB p105 functions as a processing signal for the generation of the p50 subunit. *Mol. Cell. Biol.* **16**, 2248–2254 (1996).
22. Y. Jiang *et al.*, Development of stabilized peptide-based PROTACs against estrogen receptor α. *ACS Chem. Biol.* **13**, 628–635 (2018).
23. A. Belogurov, Jr *et al.*, Multiple sclerosis autoantigen myelin basic protein escapes control by ubiquitination during proteasomal degradation. *J. Biol. Chem.* **289**, 17758–17766 (2014).
24. V. Hakim-Eshed *et al.*, Site-specific ubiquitination of pathogenic huntingtin attenuates its deleterious effects. *Proc. Natl. Acad. Sci. U.S.A.* **117**, 18661–18669 (2020).